

# Bifurcation analysis of a three-invariant, isotropic/kinematic hardening cap plasticity model for geomaterials

Richard A. Regueiro

*Materials and Engineering Sciences Center, Sandia National Laboratories, Livermore, CA 94551*

Craig D. Foster

*Department of Civil and Environmental Engineering, Stanford University, Stanford, CA 94305*

Arlo F. Fossum

*Geosciences and Environment Center, Sandia National Laboratories, Albuquerque, NM, 87185*

Ronaldo I. Borja

*Department of Civil and Environmental Engineering, Stanford University, Stanford, CA 94305*

Copyright 2004, ARMA, American Rock Mechanics Association

This paper was prepared for presentation at Gulf Rocks 2004, the 6th North America Rock Mechanics Symposium (NARMS): Rock Mechanics Across Borders and Disciplines, held in Houston, Texas, June 5-9, 2004.

This paper was selected for presentation by a NARMS Program Committee following review of information contained in an abstract submitted earlier by the author(s). Contents of the paper, as presented, have not been reviewed by ARMA/NARMS and are subject to correction by the author(s). The material, as presented, does not necessarily reflect any position of NARMS, ARMA, CARMA, SMMR, their officers, or members. Electronic reproduction, distribution, or storage of any part of this paper for commercial purposes without the written consent of ARMA is prohibited. Permission to reproduce in print is restricted to an abstract of not more than 300 words; illustrations may not be copied. The abstract must contain conspicuous acknowledgement of where and by whom the paper was presented.

**ABSTRACT:** Localized deformation such as shear bands, compaction bands, dilation bands, combined shear/compaction or shear/dilation bands, fractures, and joint slippage are commonly found in rocks. Thus, modeling their inception, development and propagation, and effect on stress response is important. This paper will focus on modeling the inception of these localized deformations—the onset of bifurcation to a localized material deformation response—for a three-invariant, isotropic/kinematic hardening cap plasticity model. Bifurcation analysis is the first step in developing a constitutive model for representing the transition of continuous rock-like material to fragmented rock material. Developing a post-bifurcation constitutive model and numerical implementation, whether via the finite element method or a meshfree method, is the next step and will not be discussed in this paper (but is part of our ongoing research). Applications of a constitutive model for modeling localized deformation in geomaterials include assessing the long term performance of nuclear waste repositories, designing tunneling construction, oil and natural gas production, and depleted reservoirs used for subsurface sequestration of greenhouse gases.

## 1. INTRODUCTION

Localized deformation such as shear bands, compaction bands, dilation bands, combined shear-compaction or shear-dilation bands, fractures, and joint slippage are commonly found in rocks. These localized deformations can be triggered by either material inhomogeneities such as joint sets in rocks, inhomogeneous stress resulting from boundary conditions such as friction at end platens in a confined compression test, or by some microstructurally driven material instability. We can account for material inhomogeneities by constitutive modeling in conjunction with a numerical simulation method such as the finite element method. Significant material inhomogeneities such as strata and joint sets can be meshed discretely, assigning different material properties for each spatial region of the finite element mesh, or they can be incorporated in an average sense

into a continuum constitutive model via directional structure/anisotropy tensors or the like. Either way, depending on boundary and loading conditions, the material deformation response predicted by the constitutive model could become mathematically unstable. This mathematical instability could be made to coincide with the natural material instability observed in the field or laboratory. The most straightforward way to do this is to endow the constitutive model with as much material characterization and representative deformation response that is deemed significant for the problem of interest. For example, if joint sets are plentiful and dominate the material deformation response, they must be represented in the constitutive model. Depending on the boundary and loading conditions, the model must predict the onset of gross localized deformation resulting from activity of certain critical joint sets. In essence, the ability of a continuum constitutive model to predict

material instability in the form of localized deformation is only as good as the model's sophistication in terms of representing material behavior. Some questions we should ask when choosing and developing constitutive models for geomaterials are: Is the material isotropic or anisotropic elastically and/or plastically? Is the material temperature and rate-sensitive? Are joint sets or other in-situ material inhomogeneities prominent?

Given a relatively sophisticated continuum constitutive model for geomaterials, this paper focuses on determining stress states at which the constitutive model predicts mathematical instabilities. With regard to modeling material deformation response after an instability is detected, such as transition of continuous rock-like material to fragmented rock material, this instability will be referred to as a bifurcation in material response. Developing a post-bifurcation constitutive model and numerical implementation, whether via the finite element method or a meshfree method, is the next step in modeling material failure in geomaterials and will not be discussed in this paper.

The bifurcation analysis assumes strong (jump in displacement) and weak (jump in strain) discontinuity kinematics for both rate insensitive and rate sensitive forms of the constitutive model. For the rate insensitive form, different bifurcation conditions result for strong and weak discontinuities as well as whether bifurcation is continuous or discontinuous. Continuous bifurcation assumes that at the instant of bifurcation there is plastic loading outside the discontinuity as well as within/on it [1]. Discontinuous bifurcation assumes there is elastic unloading outside the discontinuity and plastic loading within/on the discontinuity. Rice and Rudnicki [1] analyzed continuous and discontinuous bifurcation for weak discontinuities in the context of rate insensitive non-associative plasticity. We will extend this analysis to strong discontinuities and rate sensitivity and with future numerical examples will address specifically the effects of the third invariant and backstress on bifurcation. For weak discontinuity, we find there is a difference between continuous and discontinuous bifurcation conditions, whereas for strong discontinuity, there is no difference. We solve for the unit normal  $\mathbf{n}$  to a discontinuity interface that satisfies the loss of ellipticity condition, the determinant of the acoustic tensor  $\mathbf{A}$  is zero ( $\det \mathbf{A} = 0$ ) [2], which results from the condition that traction is continuous across the discontinuity. This bifurcation condition in essence tells us

that at a given stress state a discontinuity is admissible in our material body. This condition is necessary but not sufficient for the discontinuity to appear. It is well known in the literature that for rate sensitive plasticity, large positive values of viscosity preclude loss of ellipticity (i.e.,  $\det \mathbf{A} > 0$ ), unless the viscosity is small enough such that the model is nearly rate insensitive. Hence, loss of ellipticity is not a meaningful bifurcation condition for a rate sensitive geomaterial model. This requires us to determine a physically meaningful bifurcation condition for the rate sensitive form of the model since we know from laboratory tests and field evidence that failure occurs for rate sensitive materials. In addition, we question whether  $\det \mathbf{A} = 0$  for the rate insensitive form is a physically meaningful bifurcation condition because it depends on a continuum constitutive model and on a fit of its material parameters to data determined from homogeneously deforming experimental specimens. It seems physically meaningful to have similar bifurcation criteria for both rate insensitive and rate sensitive forms of the model. This paper, however, focuses on bifurcation analysis of rate insensitive and sensitive forms of a geomaterial constitutive model. Future work will revisit this issue.

Throughout the paper we assume small deformations and rotations. Symbolic notation is used for clearer presentation, such as the inner product of two second order tensors  $(\mathbf{a} \cdot \mathbf{b})_{ik} = a_{ij}b_{jk}$ , the contraction of two tensors  $\mathbf{a} : \mathbf{b} = a_{ij}b_{ij}$ , or the dyadic product  $(\mathbf{a} \otimes \mathbf{b})_{ijkl} = a_{ij}b_{kl}$ . Tensor operators are used such as the trace operator  $\text{tra} = a_{ii}$ , deviatoric operator  $\text{dev} \mathbf{a} = \mathbf{a} - (\text{tra} \mathbf{a} / 3) \mathbf{1}$ , symmetric gradient  $(\nabla^s \mathbf{v})_{ij} = (v_{i,j} + v_{j,i}) / 2$ , and divergence  $(\nabla \cdot \mathbf{a})_i = a_{ij,j}$ .

## 2. KINEMATICS AND GOVERNING EQUATIONS FOR WEAK AND STRONG DISCONTINUITIES

For **weak discontinuities**, we assume a planar band with thickness  $h$ , which is small relative to the size of the body (0.1% or 1%), such that  $1/h$  is a large number but remains bounded. The strain rate assuming small strains is written as [3]

$$\dot{\epsilon} = \begin{cases} \dot{\epsilon}^1 = \dot{\epsilon}^0 + \frac{1}{h} \text{sym}([\mathbf{v}] \otimes \mathbf{n}) & \in \mathcal{B}^h \\ \dot{\epsilon}^0 & \in \Omega \setminus \bar{\mathcal{B}}^h \end{cases} \quad (1)$$

where  $\dot{\epsilon} = \nabla^s \mathbf{v}$ , superscript 1 denotes just inside the band and 0 denotes just outside the band (say, across  $\mathcal{S}_+^h$ ),  $[\mathbf{v}] = \mathbf{v}_+ - \mathbf{v}_-$  is the jump in velocity across the band, and  $\mathbf{n}$  is the unit normal to the band (cf. Fig.1).

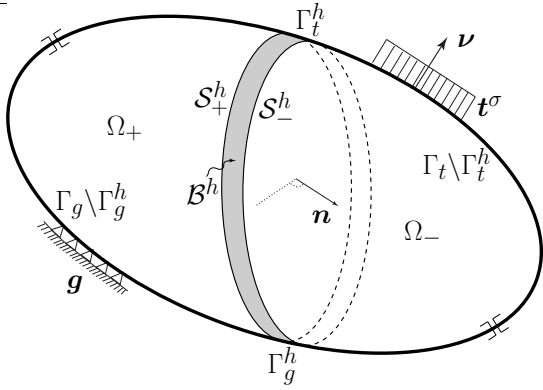


Figure 1. Body  $\bar{\Omega}$  with planar weak discontinuity  $\mathcal{B}^h$  ( $\Omega = \Omega_+ \cup \Omega_- \cup \mathcal{B}^h$ ,  $\Gamma = \Gamma_t \cup \Gamma_g \cup \mathcal{S}_+^h \cup \mathcal{S}_-^h$ ,  $\bar{\mathcal{B}}^h = \mathcal{B}^h \cup \Gamma_t^h \cup \Gamma_g^h \cup \mathcal{S}_+^h \cup \mathcal{S}_-^h$ ,  $\bar{\Omega} = \Omega \cup \Gamma$ ).

The local form of quasi-static, isothermal equilibrium for a body  $\Omega$  with weak discontinuity is written as follows

$$\begin{aligned} \nabla \cdot \boldsymbol{\sigma} + \mathbf{b} &= \mathbf{0} \quad \text{in } \Omega \\ \boldsymbol{\sigma} \cdot \boldsymbol{\nu} &= \mathbf{t}^\sigma \quad \text{on } \Gamma_t \\ \mathbf{u} &= \mathbf{g} \quad \text{on } \Gamma_g \\ \llbracket \boldsymbol{\sigma} \rrbracket \cdot \mathbf{n}_+ &= \mathbf{0} \quad \text{across } \mathcal{S}_+^h \\ \llbracket \boldsymbol{\sigma} \rrbracket \cdot \mathbf{n}_- &= \mathbf{0} \quad \text{across } \mathcal{S}_-^h \end{aligned} \quad (2)$$

where  $\boldsymbol{\sigma}$  is the Cauchy stress,  $\mathbf{b}$  is the prescribed body force,  $\boldsymbol{\nu}$  is the unit normal to  $\Gamma_t$ ,  $\mathbf{n}_+ = \mathbf{n}_- = \mathbf{n}$  is the unit normal to  $\mathcal{S}_+^h$  and  $\mathcal{S}_-^h$  since the band is assumed planar,  $\mathbf{t}^\sigma$  is the prescribed traction,  $\mathbf{g}$  is the prescribed displacement, and  $\llbracket \boldsymbol{\sigma} \rrbracket$  denotes the jump in stress across  $\mathcal{S}_+^h$  or  $\mathcal{S}_-^h$  (i.e.,  $\llbracket \boldsymbol{\sigma} \rrbracket = \boldsymbol{\sigma}^1 - \boldsymbol{\sigma}^0$ ).

The variational form of quasi-static equilibrium, using the local form as a point of departure, then may be written as follows

$$\begin{aligned} \int_{\Omega} \nabla^s \boldsymbol{\eta} : \boldsymbol{\sigma} \, d\Omega &= \int_{\Omega} \boldsymbol{\eta} \cdot \mathbf{b} \, d\Omega + \int_{\Gamma_t} \boldsymbol{\eta} \cdot \mathbf{t}^\sigma \, d\Gamma \\ &+ \int_{\mathcal{S}_+^h} \boldsymbol{\eta} \cdot (\llbracket \boldsymbol{\sigma} \rrbracket \cdot \mathbf{n}) \, d\Gamma \\ &+ \int_{\mathcal{S}_-^h} \boldsymbol{\eta} \cdot (\llbracket \boldsymbol{\sigma} \rrbracket \cdot \mathbf{n}) \, d\Gamma \end{aligned} \quad (3)$$

where  $\boldsymbol{\eta} = \delta \mathbf{u}$  is the weighting function and first variation of  $\mathbf{u}$ . The traction continuity condition  $\llbracket \boldsymbol{\sigma} \rrbracket \cdot \mathbf{n} = \mathbf{0}$  across  $\mathcal{S}_+^h$  and  $\mathcal{S}_-^h$  for a body with weak discontinuities will be used to determine bifurcation.

For **strong discontinuities**, a spatial jump in velocity  $\llbracket \mathbf{v} \rrbracket$  across  $\mathcal{S}$  leads to a singular strain rate at  $\mathcal{S}$  as [4]

$$\dot{\boldsymbol{\epsilon}} = \begin{cases} \dot{\boldsymbol{\epsilon}}^1 = \dot{\boldsymbol{\epsilon}}^0 + \text{sym}(\llbracket \mathbf{v} \rrbracket \otimes \mathbf{n}) \delta_{\mathcal{S}} & \in \mathcal{S} \\ \dot{\boldsymbol{\epsilon}}^0 & \in \Omega \setminus \mathcal{S} \end{cases} \quad (4)$$

where  $\delta_{\mathcal{S}}$  is the Dirac-delta function at the discontinuity surface  $\mathcal{S}$  (cf. Fig.2).

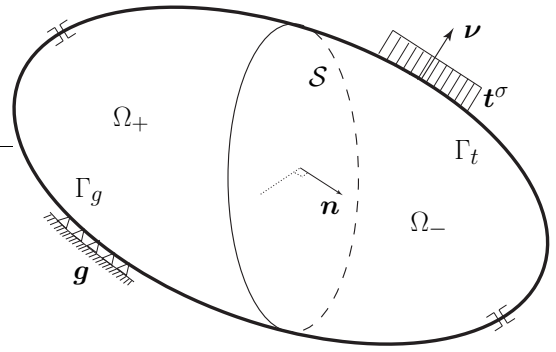


Figure 2. Body  $\bar{\Omega}$  with planar strong discontinuity  $\mathcal{S}$  ( $\Omega = \Omega_+ \cup \Omega_-$ ,  $\Gamma = \Gamma_t \cup \Gamma_g \cup \mathcal{S}$ ,  $\bar{\Omega} = \Omega \cup \Gamma$ ).

The local form of quasi-static, isothermal equilibrium for a body  $\Omega$  with strong discontinuity is written as follows

$$\begin{aligned} \nabla \cdot \boldsymbol{\sigma} + \mathbf{b} &= \mathbf{0} \quad \text{in } \Omega \\ \boldsymbol{\sigma} \cdot \boldsymbol{\nu} &= \mathbf{t}^\sigma \quad \text{on } \Gamma_t \\ \mathbf{u} &= \mathbf{g} \quad \text{on } \Gamma_g \\ \llbracket \boldsymbol{\sigma} \rrbracket \cdot \mathbf{n} &= \mathbf{0} \quad \text{across } \mathcal{S} \end{aligned} \quad (5)$$

where  $\mathbf{n}$  is the unit normal to  $\mathcal{S}$  and  $\llbracket \boldsymbol{\sigma} \rrbracket$  is the jump in stress across  $\mathcal{S}$ .

The variational form of quasi-static equilibrium is then

$$\begin{aligned} \int_{\Omega} \nabla^s \boldsymbol{\eta} : \boldsymbol{\sigma} \, d\Omega &= \int_{\Omega} \boldsymbol{\eta} \cdot \mathbf{b} \, d\Omega + \int_{\Gamma_t} \boldsymbol{\eta} \cdot \mathbf{t}^\sigma \, d\Gamma \\ &+ \int_{\mathcal{S}} \boldsymbol{\eta} \cdot (\llbracket \boldsymbol{\sigma} \rrbracket \cdot \mathbf{n}) \, d\Gamma \end{aligned} \quad (6)$$

As for weak discontinuities, the traction continuity condition  $\llbracket \boldsymbol{\sigma} \rrbracket \cdot \mathbf{n} = \mathbf{0}$  for a body with strong discontinuities will be used to determine bifurcation.

### 3. THREE-INVARIANT ISOTROPIC KINEMATIC HARDENING PLASTICITY MODEL FOR GEOMATERIALS

Here, a brief summary is given of a three-invariant isotropic/kinematic hardening cap plasticity model. For more details, refer to [5].

#### 3.1. Rate insensitive model

For small strains, an additive decomposition of the strain rate into elastic and plastic parts is assumed

$$\dot{\boldsymbol{\epsilon}} := \dot{\boldsymbol{\epsilon}}^e + \dot{\boldsymbol{\epsilon}}^p \quad (7)$$

Assuming linear isotropic elasticity, the constitutive equation for the stress rate is

$$\dot{\boldsymbol{\sigma}} = \mathbf{c}^e : \dot{\boldsymbol{\epsilon}}^e, \quad \mathbf{c}^e = \lambda \mathbf{1} \otimes \mathbf{1} + 2\mu \mathbf{I} \quad (8)$$

where  $\lambda$  and  $\mu$  are the Lamé parameters.

The single yield surface  $f$  and plastic potential function  $g$  are written in terms of the invariants as

$$f = \Gamma^2(\beta^\xi) J_2^\xi - [F_y(I_1)]^2 F_c(I_1, \kappa) = 0 \quad (9)$$

$$g = \Gamma^2(\beta^\xi) J_2^\xi - [F_y^g(I_1)]^2 F_c^g(I_1, \kappa) \quad (10)$$

where  $f$  is the yield function,  $\beta^\xi(J_2^\xi, J_3^\xi)$  is the Lode angle,  $\Gamma$  is a function of  $\beta^\xi$  and  $\Psi$  (the ratio of strength in triaxial extension versus triaxial compression,  $\Psi = 1$  if no difference in strength),  $N$  is the offset of the shear failure surface  $F_f(I_1)$  from the initial shear yield surface  $F_y(I_1) = F_f(I_1) - N$ ,  $I_1 = \sigma_{ii}$  is the first stress invariant,  $J_2^\xi = \frac{1}{2} \boldsymbol{\xi} : \boldsymbol{\xi}$  is the second invariant of the deviatoric relative stress  $\boldsymbol{\xi} = \mathbf{s} - \boldsymbol{\alpha}$ ,  $\mathbf{s}$  is the deviatoric stress,  $\boldsymbol{\alpha}$  is the deviatoric backstress associated with the Bauschinger effect,  $J_3^\xi = \frac{1}{3} (\boldsymbol{\xi} \cdot \boldsymbol{\xi}) : \boldsymbol{\xi}$  is the third invariant of the deviatoric relative stress,  $\kappa$  is the internal stress variable associated with compaction hardening,  $F_y^g(I_1) = F_f^g(I_1) - N$ , and  $g$  is the plastic potential function allowing for non-associative plastic flow. Material parameters for the shear failure surface  $F_f(I_1)$  are determined from peak stress experimental data. The purpose of the shear failure surface is to limit the hardening of the backstress  $\boldsymbol{\alpha}$ . The effect of  $F_c(I_1, \kappa)$  is to provide a smooth elliptical cap. A non-associative flow rule is assumed for plastic flow as

$$\dot{\boldsymbol{\epsilon}}^p = \dot{\gamma} \frac{\partial g}{\partial \boldsymbol{\sigma}} = \dot{\gamma} \mathbf{g} \quad (11)$$

The flow rule is associative if material parameters are chosen such that  $f = g$ . The evolution of the internal variables is

$$\begin{aligned} \dot{\boldsymbol{\alpha}} &= \dot{\gamma} \mathbf{h}^\alpha(\boldsymbol{\alpha}); \mathbf{h}^\alpha(\boldsymbol{\alpha}) = c^\alpha G^\alpha(\boldsymbol{\alpha}) \operatorname{dev} \mathbf{g} \\ \dot{\kappa} &= \dot{\gamma} h^\kappa(\kappa); h^\kappa(\kappa) = 3c^\kappa G^\kappa(\kappa) \partial g / \partial I_1 \end{aligned}$$

To determine the consistency parameter  $\dot{\gamma}$ , evaluate the consistency condition

$$\dot{f} = \frac{\partial f}{\partial \boldsymbol{\sigma}} : \dot{\boldsymbol{\sigma}} + \frac{\partial f}{\partial \boldsymbol{\alpha}} : \dot{\boldsymbol{\alpha}} + \frac{\partial f}{\partial \kappa} \dot{\kappa} = 0 \quad (12)$$

then solve for  $\dot{\gamma}$

$$\dot{\gamma} = \frac{1}{\chi} \mathbf{f} : \mathbf{c}^e : \dot{\boldsymbol{\epsilon}} \quad (13)$$

$$\chi = \mathbf{f} : \mathbf{c}^e : \mathbf{g} - \frac{\partial f}{\partial \boldsymbol{\alpha}} : \mathbf{h}^\alpha - \frac{\partial f}{\partial \kappa} h^\kappa$$

where  $\mathbf{f} = \partial f / \partial \boldsymbol{\sigma}$ . Substituting into the rate equation for stress gives

$$\dot{\boldsymbol{\sigma}} = \left( \mathbf{c}^e - \frac{1}{\chi} \mathbf{c}^e : \mathbf{g} \otimes \mathbf{f} : \mathbf{c}^e \right) : \dot{\boldsymbol{\epsilon}} = \mathbf{c}^{ep} : \dot{\boldsymbol{\epsilon}} \quad (14)$$

where  $\mathbf{c}^{ep}$  is the continuum elasto-plastic tangent.

### 3.2. Rate sensitive model

The rate sensitive form of the model involves a standard viscous regularization following Perzyna [6], which can be expressed in generalized Duvaut-Lions form [7]. The constitutive equations are similar to those of the rate insensitive model except that now there is no consistency condition by which to calculate the plastic consistency parameter (hence, regularizing the rate insensitive plasticity model).

Revisiting equations from the inviscid model, we now introduce a viscoplastic strain rate  $\dot{\boldsymbol{\epsilon}}^{vp}$  such that the evolution equations are

$$\begin{aligned} \dot{\boldsymbol{\epsilon}} &= \dot{\boldsymbol{\epsilon}}^e + \dot{\boldsymbol{\epsilon}}^{vp} \\ \dot{\boldsymbol{\sigma}} &= \mathbf{c}^e : \dot{\boldsymbol{\epsilon}} = \mathbf{c}^e : (\dot{\boldsymbol{\epsilon}} - \dot{\boldsymbol{\epsilon}}^{vp}) \\ \dot{\boldsymbol{\epsilon}}^{vp} &= \dot{\gamma} \mathbf{g} \\ \dot{\boldsymbol{\alpha}} &= \dot{\gamma} \mathbf{h}^\alpha \\ \dot{\kappa} &= \dot{\gamma} h^\kappa \\ \dot{\gamma} &= \frac{\langle g \rangle}{\eta} \end{aligned} \quad (15)$$

where  $\eta$  is the viscosity coefficient with units (Pa)<sup>3</sup>s. These equations may be expressed in generalized Duvaut-Lions form as

$$\begin{aligned} \dot{\boldsymbol{\epsilon}}^{vp} &= \frac{1}{\tau} (\mathbf{c}^e)^{-1} : (\boldsymbol{\sigma} - \bar{\boldsymbol{\sigma}}) \\ \dot{\boldsymbol{\alpha}} &= \frac{-1}{\tau} (\boldsymbol{\alpha} - \bar{\boldsymbol{\alpha}}) \\ \dot{\kappa} &= \frac{-1}{\tau} (\kappa - \bar{\kappa}) \\ \tau &= \frac{\eta}{(2\mu)^3} \end{aligned} \quad (16)$$

where  $\tau$  is the relaxation time, and  $\bar{\boldsymbol{\sigma}}, \bar{\boldsymbol{\alpha}}, \bar{\kappa}$  are solutions to the inviscid problem. The evolution equations can be written as

$$\begin{aligned} \dot{\boldsymbol{\sigma}} + \frac{1}{\tau} \boldsymbol{\sigma} &= \mathbf{c}^e : \dot{\boldsymbol{\epsilon}} + \frac{1}{\tau} \bar{\boldsymbol{\sigma}} \\ \dot{\boldsymbol{\alpha}} + \frac{1}{\tau} \boldsymbol{\alpha} &= \frac{1}{\tau} \bar{\boldsymbol{\alpha}} \\ \dot{\kappa} + \frac{1}{\tau} \kappa &= \frac{1}{\tau} \bar{\kappa} \end{aligned}$$

Since these are linear ODEs, the closed form solution may be found:

$$\begin{aligned} \boldsymbol{\sigma}(t) &= (\boldsymbol{\sigma}(0) - \bar{\boldsymbol{\sigma}}) e^{-t/\tau} + \bar{\boldsymbol{\sigma}} \\ &\quad + e^{-t/\tau} \mathbf{c}^e : \int_0^t e^{s/\tau} \dot{\boldsymbol{\epsilon}}(s) ds \end{aligned} \quad (17)$$

$$\boldsymbol{\alpha}(t) = (\boldsymbol{\alpha}(0) - \bar{\boldsymbol{\alpha}}) e^{-t/\tau} + \bar{\boldsymbol{\alpha}} \quad (18)$$

$$\kappa(t) = (\kappa(0) - \bar{\kappa}) e^{-t/\tau} + \bar{\kappa} \quad (19)$$

To obtain the inviscid solution,  $\tau \rightarrow 0$ , and to obtain the elastic solution,  $\tau \rightarrow \infty$ .

For bifurcation analysis, it is useful to express the rate sensitive form of the model in incremental form, given the inviscid solution determined from say an implicit numerical integration scheme like Backward Euler [8]. Approximating the integration in Eq.(17) leads to [6]

$$\begin{aligned}\boldsymbol{\sigma}_{n+1} &= e^{-\Delta t/\tau} \boldsymbol{\sigma}_n + (1 - e^{-\Delta t/\tau}) \bar{\boldsymbol{\sigma}}_{n+1} \\ &+ \frac{\tau}{\Delta t} (1 - e^{-\Delta t/\tau}) \mathbf{c}^e : \Delta \boldsymbol{\epsilon} \quad (20) \\ \Delta t &= t_{n+1} - t_n \\ \Delta \boldsymbol{\epsilon} &= \boldsymbol{\epsilon}_{n+1} - \boldsymbol{\epsilon}_n\end{aligned}$$

where  $t_{n+1}$  is the current time. Linearizing Eq.(20) leads to

$$\delta \boldsymbol{\sigma} = (1 - e^{-\Delta t/\tau}) \left( \delta \bar{\boldsymbol{\sigma}} + \frac{\tau}{\Delta t} \mathbf{c}^e : \delta \boldsymbol{\epsilon} \right) \quad (21)$$

where  $\mathcal{L}\boldsymbol{\sigma} = \boldsymbol{\sigma}^o + \delta \boldsymbol{\sigma}$  is the linearization operator [9].

#### 4. BIFURCATION ANALYSIS

The bifurcation analysis follows closely that conducted in [10]. As is well-reported in the literature (Sandler & Wright [11], Needleman [12], Sluys & de Borst [13]) viscous regularization in the manner of Duvaut-Lions inhibits loss of strong ellipticity for strain-softening plasticity models, assuming the viscosity is finite. For a nearly rate insensitive model (viscosity  $\eta \approx 0$ ), however, loss of strong ellipticity via the underlying inviscid model is possible. The first subsection is devoted to bifurcation analysis of the rate insensitive (inviscid) form of the model, while the second addresses bifurcation of the rate sensitive model.

##### 4.1. Rate insensitive model

We consider weak discontinuities first and then strong discontinuities, addressing both continuous and discontinuous bifurcation.

###### 4.1.1. bifurcation with weak discontinuity

For **continuous bifurcation**, plastic loading occurs outside the planar band ( $\mathbf{f} : \mathbf{c}^e : \dot{\boldsymbol{\epsilon}}^0 > 0$ ) and within the band ( $\mathbf{f} : \mathbf{c}^e : \dot{\boldsymbol{\epsilon}}^1 > 0$ ) at the instant of bifurcation. The plastic consistency parameter is assumed to decompose as (and its two parts determined from the consistency parameter derived in Eq.(13))

$$\begin{aligned}\dot{\gamma} &= \dot{\gamma} + \frac{1}{h} \dot{\gamma}_h \quad (22) \\ \dot{\gamma} &= \frac{1}{\chi} \mathbf{f} : \mathbf{c}^e : \dot{\boldsymbol{\epsilon}}^0 \\ \dot{\gamma}_h &= \frac{1}{\chi} \mathbf{f} : \mathbf{c}^e : \text{sym}([\mathbf{v}] \otimes \mathbf{n})\end{aligned}$$

Note that  $h$  is finite, and thus  $\dot{\gamma}$  is bounded. If  $h \rightarrow 0$  to make  $\dot{\gamma}$  unbounded (and, as a result, the stress-like internal state variables unbounded and the plastic dissipation undefined) then a strong discontinuity bifurcation analysis is warranted (see section 4.1.2).

At a material point, assume  $[\mathbf{v}]$  is spatially-invariant such that

$$[\mathbf{v}(t)] = \dot{\zeta}(t) \mathbf{m} \quad (23)$$

where  $\dot{\zeta}$  is the jump rate magnitude and  $\mathbf{m}$  its direction. Recall from Eq.(2) that for traction to be continuous across the planar band with normal  $\mathbf{n}$ ,  $(\dot{\boldsymbol{\sigma}}^1 - \dot{\boldsymbol{\sigma}}^0) \cdot \mathbf{n} = \mathbf{0}$  and

$$\begin{aligned}\mathbf{n} \cdot \dot{\boldsymbol{\sigma}}^0 &= \mathbf{n} \cdot \dot{\boldsymbol{\sigma}}^1 \\ \mathbf{n} \cdot \mathbf{c}^{ep} : \dot{\boldsymbol{\epsilon}}^0 &= \mathbf{n} \cdot \mathbf{c}^{ep} : \left( \dot{\boldsymbol{\epsilon}}^0 + \frac{1}{h} \text{sym}([\mathbf{v}] \otimes \mathbf{n}) \right) \\ \mathbf{0} &= \frac{\dot{\zeta}}{h} \mathbf{n} \cdot \mathbf{c}^{ep} : \mathbf{a}, \quad \mathbf{a} = \text{sym}(\mathbf{m} \otimes \mathbf{n}) \\ \mathbf{0} &= (\mathbf{n} \cdot \mathbf{c}^{ep} \cdot \mathbf{n}) \cdot \mathbf{m} = \mathbf{A} \cdot \mathbf{m} \\ \implies \det \mathbf{A} &= 0 \quad \text{for } \mathbf{m} \neq \mathbf{0} \quad (24)\end{aligned}$$

Equation (24) states that in order for there to be a nontrivial solution  $\mathbf{m} \neq \mathbf{0}$  to the traction continuity condition, the determinant of the acoustic tensor  $\mathbf{A}$  must be zero. For a given stress state  $\boldsymbol{\sigma}$  and state variables  $\alpha$  and  $\kappa$ , we solve  $\det \mathbf{A} = 0$  for the band normals  $\mathbf{n}$  and then  $\mathbf{A} \cdot \mathbf{m} = \mathbf{0}$  for the localized deformation directions.

For **discontinuous bifurcation**, there is elastic unloading outside the band ( $\mathbf{f} : \mathbf{c}^e : \dot{\boldsymbol{\epsilon}}^0 < 0$ ) and plastic loading within the band ( $\mathbf{f} : \mathbf{c}^e : \dot{\boldsymbol{\epsilon}}^1 > 0$ ). The consistency parameter is then

$$\begin{aligned}\dot{\gamma} &= \frac{1}{h} \dot{\gamma}_h \quad (25) \\ \dot{\gamma}_h &= \frac{1}{\chi} \mathbf{f} : \mathbf{c}^e : \left( h \dot{\boldsymbol{\epsilon}}^0 + \text{sym}([\mathbf{v}] \otimes \mathbf{n}) \right)\end{aligned}$$

Note that  $h$  is finite, and thus  $\dot{\gamma}$  is bounded. For traction to be continuous across the band,

$$\begin{aligned}
\mathbf{n} \cdot \dot{\boldsymbol{\sigma}}^0 &= \mathbf{n} \cdot \dot{\boldsymbol{\sigma}}^1 \\
\mathbf{n} \cdot \mathbf{c}^e : \dot{\boldsymbol{\epsilon}}^0 &= \mathbf{n} \cdot \left( \mathbf{c}^e - \frac{1}{\chi} \mathbf{c}^e : \mathbf{g} \otimes \mathbf{f} : \mathbf{c}^e \right) : \\
&\quad \left( \dot{\boldsymbol{\epsilon}}^0 + \frac{1}{h} \text{sym}(\llbracket \mathbf{v} \rrbracket \otimes \mathbf{n}) \right) \\
\mathbf{0} &= (\mathbf{n} \cdot \mathbf{c}^e \cdot \mathbf{n}) \cdot \mathbf{m} - \frac{\dot{\gamma}_h}{\dot{\zeta}} \mathbf{n} \cdot \mathbf{c}^e : \mathbf{g} \quad (26)
\end{aligned}$$

In order to determine bifurcation from Eq.(26), we need to assume a relation for  $\dot{\gamma}_h/\dot{\zeta}$ . Assuming material within the band in the post-localization regime is governed by a simple Mohr-Coulomb planar failure model, the ratio between the plastic consistency parameter  $\dot{\gamma}_h$  and shear displacement  $\dot{\zeta}$  is dependent upon the dilation/compaction angle  $\psi$  (cf. Fig. 3) as

$$\frac{\dot{\gamma}_h}{\dot{\zeta}} = \cos \psi = \mathbf{m} \cdot \mathbf{t} \quad (27)$$

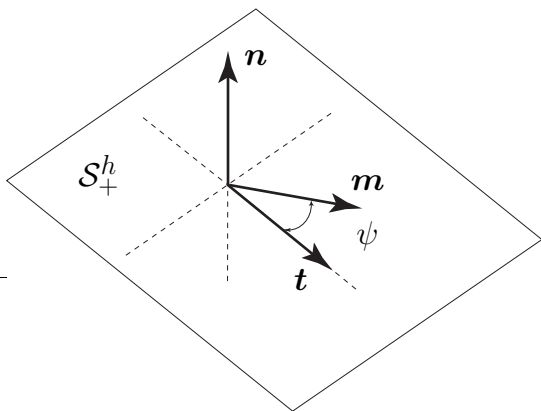


Figure 3. Band normal  $\mathbf{n}$ , tangent  $\mathbf{t}$ , and velocity jump direction  $\mathbf{m}$  with dilation/compaction angle  $\psi$ .

Then, for continuous traction across the band to be satisfied for discontinuous bifurcation,

$$\begin{aligned}
\mathbf{0} &= (\mathbf{n} \cdot \mathbf{c}^e \cdot \mathbf{n}) \cdot \mathbf{m} - (\mathbf{m} \cdot \mathbf{t}) \mathbf{n} \cdot \mathbf{c}^e : \mathbf{g} \\
\mathbf{0} &= [\mathbf{n} \cdot \mathbf{c}^e \cdot \mathbf{n} - (\mathbf{n} \cdot \mathbf{c}^e : \mathbf{g}) \otimes \mathbf{t}] \cdot \mathbf{m} \\
\mathbf{0} &= \hat{\mathbf{A}} \cdot \mathbf{m} \\
\implies \det \hat{\mathbf{A}} &= 0 \quad \text{for } \mathbf{m} \neq \mathbf{0} \quad (28)
\end{aligned}$$

Notice the bifurcation conditions for continuous and discontinuous bifurcation in Eqs.(24) and (28), respectively, are different for the case of weak discontinuity, regardless of the assumption made in Eq.(27). It is interesting to note that given the assumption in Eq.(27), if we have a pure dilation/compaction band (i.e.,  $\mathbf{m} \cdot \mathbf{t} = 0$ ), then discontinuous bifurcation for weak discontinuity is not possible since  $\mathbf{c}^e$  is positive definite (see Eq. (28)).

We will show that for the case of strong discontinuity, the bifurcation conditions are the same for continuous and discontinuous bifurcation.

#### 4.1.2. bifurcation with strong discontinuity

Recall the planar surface is of zero measure, such that the velocity field is discontinuous across  $\mathcal{S}$  [4]. For **continuous bifurcation**, the plastic consistency parameter is decomposed as

$$\dot{\gamma} = \dot{\bar{\gamma}} + \dot{\gamma}_\delta \delta_{\mathcal{S}} \quad (29)$$

In order for the backstress and isotropic stress to be bounded (and the plastic dissipation to be well-defined [4]), the hardening moduli  $c^\alpha$  and  $c^\kappa$  bifurcate

$$\begin{aligned}
(c^\alpha)^{-1} &= (\bar{c}^\alpha)^{-1} + (c_\delta^\alpha)^{-1} \delta_{\mathcal{S}} \quad (30) \\
(c^\alpha)^{-1} \dot{\boldsymbol{\alpha}} &= G^\alpha \dot{\gamma} \text{dev} \mathbf{g} \\
\dot{\boldsymbol{\alpha}} &= \bar{c}^\alpha G^\alpha \dot{\bar{\gamma}} \text{dev} \mathbf{g} = \bar{\mathbf{h}}^\alpha \dot{\bar{\gamma}} \\
\dot{\boldsymbol{\alpha}} &= c_\delta^\alpha G^\alpha \dot{\gamma}_\delta \text{dev} \mathbf{g} = \mathbf{h}_\delta^\alpha \dot{\gamma}_\delta
\end{aligned}$$

$$\begin{aligned}
(c^\kappa)^{-1} &= (\bar{c}^\kappa)^{-1} + (c_\delta^\kappa)^{-1} \delta_{\mathcal{S}} \quad (31) \\
(c^\kappa)^{-1} \dot{\kappa} &= G^\kappa \dot{\gamma} \text{tr} \mathbf{g} \\
\dot{\kappa} &= \bar{c}^\kappa G^\kappa \dot{\bar{\gamma}} \text{tr} \mathbf{g} = \bar{h}^\kappa \dot{\bar{\gamma}} \\
\dot{\kappa} &= c_\delta^\kappa G^\kappa \dot{\gamma}_\delta \text{tr} \mathbf{g} = h_\delta^\kappa \dot{\gamma}_\delta
\end{aligned}$$

Then, the consistency condition reads

$$\begin{aligned}
\dot{f} &= \mathbf{f} : \mathbf{c}^e : (\dot{\boldsymbol{\epsilon}}^0 + \dot{\zeta} \mathbf{a} \delta_{\mathcal{S}} - (\dot{\bar{\gamma}} + \dot{\gamma}_\delta \delta_{\mathcal{S}}) \mathbf{g}) \\
&\quad + \frac{\partial f}{\partial \boldsymbol{\alpha}} : \bar{\mathbf{h}}^\alpha \dot{\bar{\gamma}} + \frac{\partial f}{\partial \kappa} \bar{h}^\kappa \dot{\bar{\gamma}} = 0 \quad (32)
\end{aligned}$$

and for the regular and singular parts of the consistency condition to be satisfied,

$$\begin{aligned}
\dot{\bar{\gamma}} &= \frac{1}{\bar{\chi}} \mathbf{f} : \mathbf{c}^e : \dot{\boldsymbol{\epsilon}}^0 \\
\bar{\chi} &= \mathbf{f} : \mathbf{c}^e : \mathbf{g} - \frac{\partial f}{\partial \boldsymbol{\alpha}} : \bar{\mathbf{h}}^\alpha - \frac{\partial f}{\partial \kappa} \bar{h}^\kappa \\
\dot{\gamma}_\delta &= \frac{\mathbf{f} : \mathbf{c}^e : \text{sym}(\llbracket \mathbf{v} \rrbracket \otimes \mathbf{n})}{\mathbf{f} : \mathbf{c}^e : \mathbf{g}}
\end{aligned}$$

Then the stress rate on the surface  $\mathcal{S}$ ,  $\dot{\boldsymbol{\sigma}}^1$ , and outside the surface,  $\dot{\boldsymbol{\sigma}}^0$ , read

$$\begin{aligned}
\dot{\boldsymbol{\sigma}}^1 &= \underbrace{\left( \mathbf{c}^e - \frac{1}{\bar{\chi}} \mathbf{c}^e : \mathbf{g} \otimes \mathbf{f} : \mathbf{c}^e \right)}_{\bar{\mathbf{c}}^{ep}} : \dot{\boldsymbol{\epsilon}}^0 \\
&\quad + \dot{\zeta} \underbrace{\left( \mathbf{c}^e - \frac{\mathbf{c}^e : \mathbf{g} \otimes \mathbf{f} : \mathbf{c}^e}{\mathbf{f} : \mathbf{c}^e : \mathbf{g}} \right)}_{\bar{\mathbf{c}}^{ep}} : \mathbf{a} \delta_{\mathcal{S}} \quad (33)
\end{aligned}$$

$$\dot{\boldsymbol{\sigma}}^0 = \bar{\mathbf{c}}^{ep} : \dot{\boldsymbol{\epsilon}}^0 \quad (34)$$

For continuous traction across the discontinuity surface

$$\begin{aligned} \mathbf{n} \cdot \dot{\boldsymbol{\sigma}}^0 &= \mathbf{n} \cdot \dot{\boldsymbol{\sigma}}^1 \\ \mathbf{n} \cdot \tilde{\mathbf{c}}^{ep} : \dot{\boldsymbol{\epsilon}}^0 &= \mathbf{n} \cdot \tilde{\mathbf{c}}^{ep} : \dot{\boldsymbol{\epsilon}}^0 + \dot{\zeta} \mathbf{n} \cdot \tilde{\mathbf{c}}^{ep} : \mathbf{a} \delta_S \\ \mathbf{0} &= (\mathbf{n} \cdot \tilde{\mathbf{c}}^{ep} \cdot \mathbf{n}) \cdot \mathbf{m} \delta_S = \tilde{\mathbf{A}} \cdot \mathbf{m} \delta_S \\ &\implies \det \tilde{\mathbf{A}} = 0 \quad \text{for } \mathbf{m} \neq \mathbf{0} \end{aligned} \quad (35)$$

For **discontinuous bifurcation**, the consistency parameter is localized to the discontinuity as

$$\dot{\gamma} = \dot{\gamma}_\delta \delta_S \quad (36)$$

Again, the hardening moduli bifurcate in order to have well defined plastic dissipation. Then, the consistency condition reads

$$\begin{aligned} \dot{f} &= \mathbf{f} : \mathbf{c}^e : (\dot{\boldsymbol{\epsilon}}^0 + \dot{\zeta} \mathbf{a} \delta_S - \dot{\gamma}_\delta \mathbf{g} \delta_S) \\ &+ \frac{\partial f}{\partial \boldsymbol{\alpha}} : \mathbf{h}_\delta^\alpha \dot{\gamma}_\delta + \frac{\partial f}{\partial \kappa} h_\delta^\kappa \dot{\gamma}_\delta = 0 \end{aligned} \quad (37)$$

and for the regular and singular parts of the consistency condition to be satisfied,

$$\dot{\gamma}_\delta = \frac{-\mathbf{f} : \mathbf{c}^e : \dot{\boldsymbol{\epsilon}}^0}{\frac{\partial f}{\partial \boldsymbol{\alpha}} : \mathbf{h}_\delta^\alpha + \frac{\partial f}{\partial \kappa} h_\delta^\kappa} = \frac{\dot{\zeta} \mathbf{f} : \mathbf{c}^e : \mathbf{a}}{\mathbf{f} : \mathbf{c}^e : \mathbf{g}} \quad (38)$$

For continuous traction across the discontinuity surface  $\mathcal{S}$

$$\begin{aligned} \mathbf{n} \cdot \dot{\boldsymbol{\sigma}}^0 &= \mathbf{n} \cdot \dot{\boldsymbol{\sigma}}^1 \\ \mathbf{n} \cdot \mathbf{c}^e : \dot{\boldsymbol{\epsilon}}^0 &= \mathbf{n} \cdot \mathbf{c}^e : \dot{\boldsymbol{\epsilon}}^0 + \dot{\zeta} \mathbf{n} \cdot \tilde{\mathbf{c}}^{ep} : \mathbf{a} \delta_S \\ \mathbf{0} &= \tilde{\mathbf{A}} \cdot \mathbf{m} \delta_S \\ &\implies \det \tilde{\mathbf{A}} = 0 \quad \text{for } \mathbf{m} \neq \mathbf{0} \end{aligned}$$

Thus, the same bifurcation condition results for continuous and discontinuous bifurcation for the case of strong discontinuity localized kinematics.

## 4.2. Rate sensitive model

### 4.2.1. weak discontinuity

For **continuous bifurcation**, from Eq.(17), the stress just outside and just inside the band are, respectively,

$$\begin{aligned} \boldsymbol{\sigma}^0(t) &= (\boldsymbol{\sigma}^0(0) - \bar{\boldsymbol{\sigma}}^0) e^{-t/\tau} + \bar{\boldsymbol{\sigma}}^0 \\ &+ e^{-t/\tau} \mathbf{c}^e : \int_0^t e^{s/\tau} \dot{\boldsymbol{\epsilon}}^0(s) ds \end{aligned} \quad (39)$$

$$\begin{aligned} \boldsymbol{\sigma}^1(t) &= (\boldsymbol{\sigma}^1(0) - \bar{\boldsymbol{\sigma}}^1) e^{-t/\tau} + \bar{\boldsymbol{\sigma}}^1 \\ &+ e^{-t/\tau} \mathbf{c}^e : \int_0^t e^{s/\tau} \dot{\boldsymbol{\epsilon}}^1(s) ds \end{aligned} \quad (40)$$

where, recall,  $\bar{\boldsymbol{\sigma}}$  denotes inviscid stress, and we assume at time zero that the stresses just inside and just

outside the band are equal  $\boldsymbol{\sigma}^0(0) = \boldsymbol{\sigma}^1(0)$ . Then, for continuous traction across the band,

$$\begin{aligned} \mathbf{n} \cdot \boldsymbol{\sigma}^0(t) &= \mathbf{n} \cdot \boldsymbol{\sigma}^1(t) \\ \mathbf{0} &= \mathbf{n} \cdot (\bar{\boldsymbol{\sigma}}^1 - \bar{\boldsymbol{\sigma}}^0)(1 - e^{-t/\tau}) \\ &+ \frac{1}{h} e^{-t/\tau} \mathbf{n} \cdot \mathbf{c}^e : \mathbf{a} \int_0^t e^{s/\tau} \dot{\zeta}(s) ds \\ \tau \rightarrow 0 &\implies \mathbf{n} \cdot (\bar{\boldsymbol{\sigma}}^1 - \bar{\boldsymbol{\sigma}}^0) = \mathbf{0} \\ \tau \rightarrow \infty &\implies (\mathbf{n} \cdot \mathbf{c}^e \cdot \mathbf{n}) \cdot \mathbf{m} = \mathbf{0} \end{aligned} \quad (41)$$

As expected, for  $\tau \rightarrow 0$  we obtain the bifurcation condition for the inviscid case, and for  $\tau \rightarrow \infty$ , we obtain the elastic solution and hence no loss of strong ellipticity (real, elastic wave speeds, after Hadamard, cf. Hill [14]). The lower bound ( $\tau \rightarrow 0$ ) on the viscous bifurcation condition is useful in that if a geomaterial is nearly rate insensitive even when loaded to high strain rates, its bifurcation will depend on an analysis of the inviscid model. Then, the dynamic characteristics of the crack/shear band propagation and post-localization constitutive response will be important even for a nearly rate insensitive geomaterial.

For a rate sensitive geomaterial, not so highly viscous to be elastic ( $\tau > 0$  is finite), there should be no bifurcation to localized deformation mode; see Eq.(41). This should be made clear by an analysis for the discrete form of the integrated equations, as in section 4.2.3.

For **discontinuous bifurcation**, the analysis is the same as for continuous bifurcation, except that the inviscid stress jump across the band interface such as  $S_+^h, \bar{\boldsymbol{\sigma}}^1 - \bar{\boldsymbol{\sigma}}^0$ , is different.

### 4.2.2 strong discontinuity

For strong discontinuities, bifurcation analysis of the viscoplastic model is the same as for weak discontinuities, except of course that the inviscid bifurcation analysis is different as shown above in the analysis of the rate insensitive model.

### 4.2.3 discrete form of rate sensitive model

Bifurcation analysis of the discrete form of a rate sensitive model allows one to analyze acoustic tensors to determine mathematical instability.

In linearized form, the incremental strain for **weak discontinuity** comes from Eq.(1). For continuous bifurcation, from Eq.(14), the incremental stress for the inviscid solution is given, and from Eq.(21), the incremental stress for the viscous solution is

$$\delta \boldsymbol{\sigma}^0 = \underbrace{(1 - e^{-\Delta t/\tau}) \left( \mathbf{c}^{ep} + \frac{\tau}{\Delta t} \mathbf{c}^e \right)}_{\hat{\mathbf{c}}^{ep}} : \delta \boldsymbol{\epsilon}^0 \quad (42)$$

$$\delta\boldsymbol{\sigma}^1 = \hat{\mathbf{c}}^{ep} : \delta\boldsymbol{\epsilon}^1$$

Then for continuous traction,

$$\begin{aligned} \mathbf{n} \cdot \delta\boldsymbol{\sigma}^0 &= \mathbf{n} \cdot \delta\boldsymbol{\sigma}^1 \\ \mathbf{n} \cdot \hat{\mathbf{c}}^{ep} : \delta\boldsymbol{\epsilon}^0 &= \mathbf{n} \cdot \hat{\mathbf{c}}^{ep} : \delta\boldsymbol{\epsilon}^0 + \frac{\delta\zeta}{h} \mathbf{n} \cdot \hat{\mathbf{c}}^{ep} : \mathbf{a} \\ \mathbf{0} &= (\mathbf{n} \cdot \hat{\mathbf{c}}^{ep} \cdot \mathbf{n}) \mathbf{m} = \hat{\mathbf{A}} \cdot \mathbf{m} \\ \tau \rightarrow 0 &\implies \hat{\mathbf{c}}^{ep} = \mathbf{c}^{ep} \\ \tau \rightarrow \infty &\implies \hat{\mathbf{c}}^{ep} = \mathbf{c}^e \end{aligned}$$

and for finite  $\tau > 0$ ,  $\hat{\mathbf{c}}^{ep}$  should remain positive definite, i.e.  $\det \hat{\mathbf{A}} > 0$ , but more analysis is needed to determine this. For discontinuous bifurcation, the incremental form for the inviscid solution along with the incremental viscous solution gives for continuous traction,

$$\begin{aligned} \mathbf{n} \cdot \delta\boldsymbol{\sigma}^0 &= \mathbf{n} \cdot \delta\boldsymbol{\sigma}^1 \\ \mathbf{0} &= -(1 - e^{-\Delta t/\tau}) \\ &\quad \times \left( \frac{\mathbf{f} : \mathbf{c}^e : \delta\boldsymbol{\epsilon}^0}{\chi} \right) \mathbf{n} \cdot \mathbf{c}^e : \mathbf{g} \\ &\quad + \frac{\delta\zeta}{h} \mathbf{n} \cdot \hat{\mathbf{c}}^{ep} : \mathbf{a} \\ \tau \rightarrow 0 &\implies \text{inviscid} \\ \tau \rightarrow \infty &\implies \text{elastic} \end{aligned}$$

and for finite  $\tau > 0$ , the analysis is inconclusive.

For **strong discontinuity**, the incremental strain from Eq.(4) is given. For continuous bifurcation, the incremental form of the inviscid solution comes from Eqs.(33) and (34) and then for continuous traction,

$$\begin{aligned} \mathbf{n} \cdot \delta\boldsymbol{\sigma}^0 &= \mathbf{n} \cdot \delta\boldsymbol{\sigma}^1 \\ \mathbf{0} &= (\mathbf{n} \cdot \hat{\mathbf{c}}^{ep} \cdot \mathbf{n}) \cdot \mathbf{m} \delta_S = \hat{\mathbf{A}} \cdot \mathbf{m} \delta_S \\ \tau \rightarrow 0 &\implies \hat{\mathbf{c}}^{ep} = \tilde{\mathbf{c}}^{ep} \\ \tau \rightarrow \infty &\implies \hat{\mathbf{c}}^{ep} = \mathbf{c}^e \end{aligned}$$

where here  $\hat{\mathbf{c}}^{ep}$  is a function of  $\tilde{\mathbf{c}}^{ep}$  rather than  $\mathbf{c}^{ep}$  in Eq.(42). For finite  $\tau > 0$ ,  $\hat{\mathbf{c}}^{ep}$  should remain positive definite, i.e. that  $\det \hat{\mathbf{A}} > 0$ , but more analysis is needed. For discontinuous bifurcation, the same bifurcation condition for  $\tau \rightarrow 0$  results as for continuous bifurcation with strong discontinuity.

#### 4.3 Effects of third invariant and backstress

Effects of the third invariant  $J_3^\xi$  and backstress  $\boldsymbol{\alpha}$  on bifurcation are embedded within the tangents  $\mathbf{c}^{ep}$ ,  $\hat{\mathbf{c}}^{ep}$ , and  $\tilde{\mathbf{c}}^{ep}$ .

Numerical examples are forthcoming that will demonstrate the effect of the third invariant and backstress on bifurcation.

## 5. CONCLUSIONS

One conclusion of this paper is that for a rate insensitive model, bifurcation conditions under weak discontinuity for continuous and discontinuous bifurcation are different whereas they are the same under strong discontinuity. This result for strong discontinuity stems from bifurcation of the hardening moduli that leads to an elastic-perfectly-plastic acoustic tensor [4]. For determining mathematical instability for weak discontinuities, however, it was shown in [1] that continuous bifurcation provides the lower bound for the range of discontinuous bifurcation, and thus is the more critical condition. For a rate sensitive model, it is unsurprising that for large viscosity, mathematical stability is ensured even for strain-softening plasticity. But for smaller values of viscosity, the bifurcation analysis is inconclusive whether mathematical instability will occur or not. Future numerical examples will address this question.

## 6. ACKNOWLEDGEMENTS

Sandia is a multiprogram laboratory operated by Sandia Corporation, a Lockheed Martin Company, for the United States Department of Energy under contract DE-ACO4-94AL85000.

## REFERENCES

- [1] Rice, J.R. and J.W. Rudnicki. 1980. A note on some features of the theory of localization of deformation. *Int. J. Solids Struct.* 16: 597–605.
- [2] Rudnicki, J.W. and J.R. Rice. 1975. Conditions for the localization of deformation in pressure-sensitive dilatant materials. *J. Mech. Phys. Solids.* 23: 371–394.
- [3] Borja, R.I. 2002. Bifurcation of elastoplastic solids to shear band mode at finite strain. *Comput. Methods Appl. Mech. Engrg.* 191: 5287–5314.
- [4] Simo, J.C., J. Oliver, and F. Armero. 1993. An analysis of strong discontinuities induced by strain-softening in rate-independent inelastic solids. *Comput. Mech.* 12: 277–296.
- [5] Fossum, A.F. and J.T. Fredrich. 2000. Cap plasticity models and compactive and dilatant pre-failure deformation. In *Pacific Rocks 2000: Rock Around the Rim*, eds. J. Girard et al., 1169–1176. A.A. Balkema.
- [6] Simo, J.C. and T.J.R. Hughes. 1998. *Computational Inelasticity*, Springer Verlag New York, Inc.
- [7] Duvaut, G. and J.L. Lions. 1972. *Les Inequations en Mecanique et en Physique*, Dunod, Paris.
- [8] Foster, C.D., R.A. Regueiro, A.F. Fossum, and R.I. Borja. 2004. Implicit numerical integration of a three-invariant, isotropic/kinematic hardening cap plasticity model for geomaterials. in preparation.

- [9] Marsden, J.E. and T.J.R. Hughes. 1983. *Mathematical Foundations of Elasticity*. Prentice-Hall.
- [10] Borja, R.I. and A. Aydin. 2004. Computational modeling of deformation bands in granular media, I: Geological and mathematical framework. *Comput. Methods Appl. Mech. Engrg.* in press.
- [11] Sandler, I.S. and J.P. Wright. 1984. Strain-softening. In *Theoretical Foundations for Large Scale Computations of Nonlinear Material Behavior*, eds. S. Nemat-Nasser et al., 285–315, Martinus Nijhoff Pub., The Netherlands.
- [12] Needleman, A. 1988. Material rate dependence and mesh sensitivity in localization problems. *Comput. Methods Appl. Mech. Engrg.* 67: 69–85.
- [13] Sluys, L.J. and R. de Borst. 1992. Wave propagation and localization in a rate-dependent cracked medium: Model formulation and one-dimensional examples. *Int. J. Solids Struct.* 29: 2945–2958.
- [14] Hill, R. 1962. Acceleration waves in solids. *J. Mech. Phys. Solids.* 10: 1–16.
- [15] Borja, R.I. 2004. Computational modeling of deformation bands in granular media, II: Numerical simulations. *Comput. Methods Appl. Mech. Engrg.* in press.